Synthesis, Swelling Behavior, and Biocompatibility of Novel Physically Cross-Linked Polyurethane-*block*-Poly(glycerol methacrylate) Hydrogels

Kibret Mequanint,*[,†,‡] Alpesh Patel,[†] and Deon Bezuidenhout[§]

Department of Chemical and Biochemical Engineering, and Graduate Program in Biomedical Engineering, University of Western Ontario, London, Ontario N6A 5B9, Canada, and Cardiovascular Research Unit, Department of Cardiothoracic Surgery, University of Cape Town, Observatory 7925, Cape Town, South Africa

Received September 22, 2005; Revised Manuscript Received December 21, 2005

Physically cross-linked novel block copolymer hydrogels with tunable hydrophilic properties for biomedical applications were synthesized by controlled radical polymerization of polyurethane macroiniferter and (2,2-dimethyl-1,3-dioxolane) methyl methacrylate. The block copolymers were converted to hydrogels by the selective hydrolysis of poly[(2,2-dimethyl-1,3-dioxolane) methyl methacrylate] block to poly(glycerol methacrylate). The block copolymerization has been monitored by monomer conversion and molecular weight increase as a function of time. It was observed that the polymerization proceeded with a characteristic "living" behavior where both monomer conversion and molecular weight increased linearly, with increasing reaction time. The resulting hydrogels were investigated for their equilibrium water content (EWC), dynamic water contact angles, swelling kinetics, thermodynamic interaction parameters, plasma protein adsorption, and platelet adhesion. Similar to our previous mechanically responsive hydrogels (Mequanint, K.; Sheardown, H. *J. Biomater. Sci. Polym. Ed.* **2005**, *10*, 1303−1318), the present results indicated that block copolymer hydrogels have excellent hydrophilicity and swelling behavior with improved modulus of elasticity. The equilibrium swelling was affected by the hydrolysis time, block length of poly(glycerol methacrylate), temperature, and the presence of soluble salts. Fibrinogen adsorption and platelet adhesion were significantly lower for the hydrogels than for the control polyurethane, whereas albumin adsorption increased for the hydrogels in proportion to the contents of poly(glycerol methacrylate). These hydrogels have potential in a number of biomedical applications such as drug delivery and scaffolds for tissue engineering.

Introduction

The ability of polymers to undergo substantial swelling when exposed to an aqueous environment constitutes the generic definition of hydrogels. Such swelling, which accompanies a change in volume of the material, can further be induced by temperature, pH, ionic strength, and pressure.[1] The biomedical applications of hydrogels (the ability to release drugs in a sustained manner, the high permeability to allow metabolic products to be removed, the slippery effect that reduces frictional irritation to the surrounding tissues and low interfacial tension with body fluids that can reduce the tendency of proteins to be adsorbed, and their ability to be fabricated into a large number of shapes) is linked to their swelling ability. Because of these properties, hydrogels find valuable applications for suture and catheter coatings, contact lenses, drug delivery vehicles, scaffolds for tissue engineering, and artificial organs.

Because linear hydrogels tend to dissolve rather than swell in water and possess poor mechanical properties, most hydrogels are cross-linked using multifunctional cross-linkers.[2] Cross-linking is often done in the synthesis stage, and this has a disadvantage as the resulting device cannot be reshaped or resized since the polymer is no longer soluble in solvents and heating to melt-process can only degrade the polymer once cross-linking took place. Clearly, it would be desirable to design linear hydrogel biomaterials that cannot be dissolved in water but can be processed using organic solvents. Such hydrogels are beneficial for ease of fabrication and postprocess modifications. A linear water-swellable polymer that can be dissolved in organic solvents is easy to fabricate into any size and shape as well as allows melting and extrusion techniques to be used for device manufacturing.

Recently, there has been interest in linear hydrogels for biomedical applications. The work done by Li and co-workers on the synthesis of triblock PLA-*block*-PEO-*block*-PLA copolymer hydrogels by ring opening polymerization for protein drug delivery application is an example of this interest.[3] In a series of papers, Huglin and co-workers synthesized physically cross-linked hydrogels based on random copolymers of *N*-vinyl-2-pyrolidone and methyl methacrylate.[4,5] Other physically cross-linked random copolymer hydrogels have also been reported by Devine [6] and Muratore.[7] Since the major limitation of hydrogels for biomedical applications is their poor mechanical properties, our previous publication demonstrated the incorporation of urethane functionality into a hydrophilic polymer to improve the mechanical properties of an otherwise weak hydrogel system.[8] In a different approach Petrini and co-workers reported a series of linear polyurethane hydrogels based on poly(ethylene oxide) soft segment that had high equilibrium water content (ca. >100%).[9] Since the water content of most tissues

* To whom correspondence should be addressed. E-mail: kmequani@eng.uwo.ca. Tel: +1 (519) 661-2111 ext. 88573. Fax: +1 (519) 661-3498.

† Department of Chemical and Biochemical Engineering, University of Western Ontario.

‡ Graduate Program in Biomedical Engineering, University of Western Ontario.

§ University of Cape Town.

10.1021/bm0507047 CCC: $33.50
Published on Web 02/18/2006

Scheme 1. Syntheses of (a) 1,1,2,2-Tetraphenyl-1,2-ethanediol (TPED) Iniferter and (b) Solketal Methacrylate (SMA)

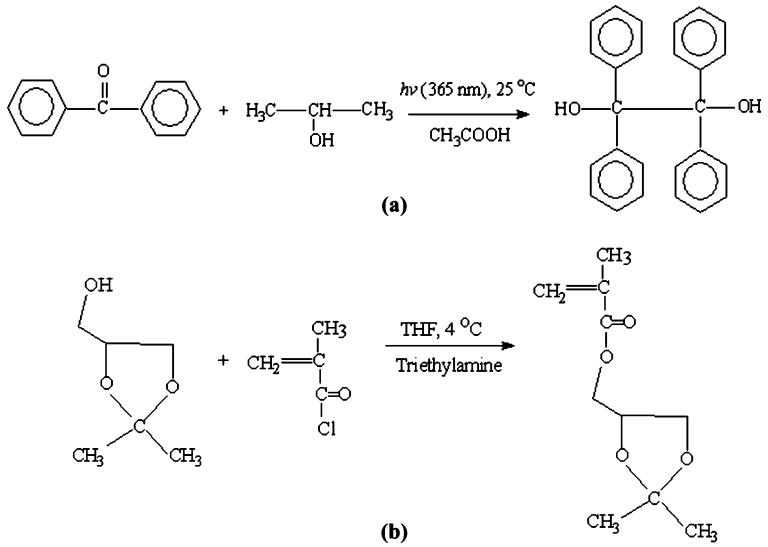

is well below this value, the design of linear hydrogel biomaterials that mimic the water content of natural tissues (20−80%) is required. The lower water content of hydrogels also improves their mechanical properties, one of the challenges in designing swellable polymers.[10]

Recent advances made in controlled polymerization techniques allowed the design of tailored biomaterials with desired composition and chain lengths.[11] One of the controlled polymerization techniques that could employ polyurethanes is the macroiniferter method.[12,13] The term iniferter is a combination of initiator, transfer agent and terminator and is used to describe a group of compounds which thermally or photochemically initiate the polymerization of vinyl monomers, reversibly convert the growing polymers into dormant ones, and eventually participate in the termination of the growing chains.[11] A macroiniferter is therefore a polymeric iniferter. In this method, tailored polyurethane block copolymer hydrogels with the required hydrophobic/hydrophilic block lengths can be potentially synthesized thus allowing desired properties to be customized. However, polyurethane (PU) block copolymer hydrogel biomaterials made by the macroiniferter technique have not been reported so far.

In this paper, we report the synthesis, swelling behavior, and biocompatibility of novel linear polyurethane-*block*-poly(glycerol methacrylate) hydrogels based on polytetramethylene oxide (PTMO, $M_w = 2000$) and (2,2-dimethyl-1,3-dioxolane) methyl methacrylate.

Experimental Section

Chemicals. All chemicals were purchased from Sigma-Aldrich (Milwaukee, WI). Tetrahydrofuran (THF) and dimethylformamide (DMF) were distilled at a reduced pressure of 26 KPa and the middle fraction was stored at 4 °C until used. Polytetramethylene oxide (PTMO, $M_w = 2000$) was dried at 90 °C and reduced pressure until it was bubble free. 4,4′-Diphenylmethane diisocyanate (MDI) was purified by hot filtration, whereas triethylamine, 2,2-dimethyl-1,3-dioxolane-4 methanol (commonly, and hereafter called solketal), methacryloyl chloride, dibutyltindilaurate (DBTL), 2-propanol, glacial acetic acid, and benzophenone were used as received. All other precipitating solvents were also used as received.

Synthesis of 1,1,2,2-Tetraphenyl-1,2-ethanediol (TPED) Iniferter. Benzophenone (0.1 mol; 18.2 g) and 5-fold molar excess 2-propanol in the presence of glacial acetic acid (0.005 mol; 0.03 g) were mixed. The mixture was assembled in a 500 mL round-bottom flask and exposed to 365 nm UV light (model B100AP from UVP Inc., Upland, CA). TPED precipitated as it was formed. The precipitated product was purified by re-crystallization from acetic acid and stored at 4 °C until used (Scheme 1a).

Synthesis of (2,2-Dimethyl-1,3-dioxolane) Methyl Methacrylate. (2,2-Dimethyl-1,3-dioxolane) methyl methacrylate, commonly and hereafter called solketal methacrylate (SMA), was synthesized from 2,2-dimethyl-1,3-dioxolane-4-methanol (commonly called solketal) and methacryloyl chloride.[14] Solketal (0.5 mol, 66 g), triethylamine (0.5 mol), and 200 mL of THF were added to a 500 mL round-bottom reaction flask, and the flask was purged with nitrogen and sealed. Methacryloyl chloride (0.6 mol, 62.4 g) was injected into the flask using a hypodermic needle, via a rubber septum, while the temperature was kept at 4 °C in an ice bath. The mixture was stirred using a stir bar for 10 h after which the temperature was slowly raised to room temperature and stirred for a further 10 h under nitrogen atmosphere. The reaction product was filtered to remove the triethylamine hydrochloride salt, which was already precipitated. The solution was washed with saturated sodium chloride and dried with anhydrous sodium carbonate (Scheme 1b). SMA (85 g, 66% yield) obtained as a colorless liquid was passed through an inhibitor-removing column. ^{1}H NMR (chloroform-d): δ 6.11 ppm (s, 1H, C═CH trans), 5.62 ppm (s, 1H, C═CH cis), 3.71−4.52 ppm (m, 5H, O−CH_2CHCH_2), 1.96 ppm (s, 3H, ═C−CH_3), 1.38−1.45 ppm (d, 6H, −C(CH_3)$_2$).

Synthesis of Segmented Polyurethane Macroiniferter (PUMI). A 1-L glass reactor equipped with heating element, a mechanical stirrer, a charging and sampling port, and a nitrogen inlet and outlet was charged with PTMO 2000 (50% solution in THF) and MDI in 1:2 molar ratio. The reaction took place at 65 °C over 2.5 h. After 2.5 h, the temperature was reduced to 35 °C, and stoichiometric amounts of TPED and 0.2% DBTL (based on the isocyanate content) were added and allowed to react with the isocyanate (−NCO) for 12 h. Progress and completion of the reaction were monitored by measuring the disappearance of the isocyanate peak by means of FTIR at 2265 cm^{-1}. The PUMI was then precipitated in a water−methanol mixture (1:1 v/v), washed twice in distilled water, and dried in a vacuum oven at 30 °C.

Synthesis of PU-*block*-PSMA Polymers. PUMI (5 g; 25% in DMF) and SMA (6.5 g) were charged in a 250 mL round-bottom reaction flask equipped with a magnetic stirrer and heater. Nitrogen was bubbled through the reactor to remove dissolved oxygen, and the contents were sealed. The flask was then heated to 65−85 °C to initiate the reaction and obtain PU-*b*-PSMA polymers. For a given polymerization tem-

Scheme 2. Syntheses of PUMI, PU-*b*-PSMA and the Corresponding PU-*b*-PGMA Xerogels by Selective Hydrolysis

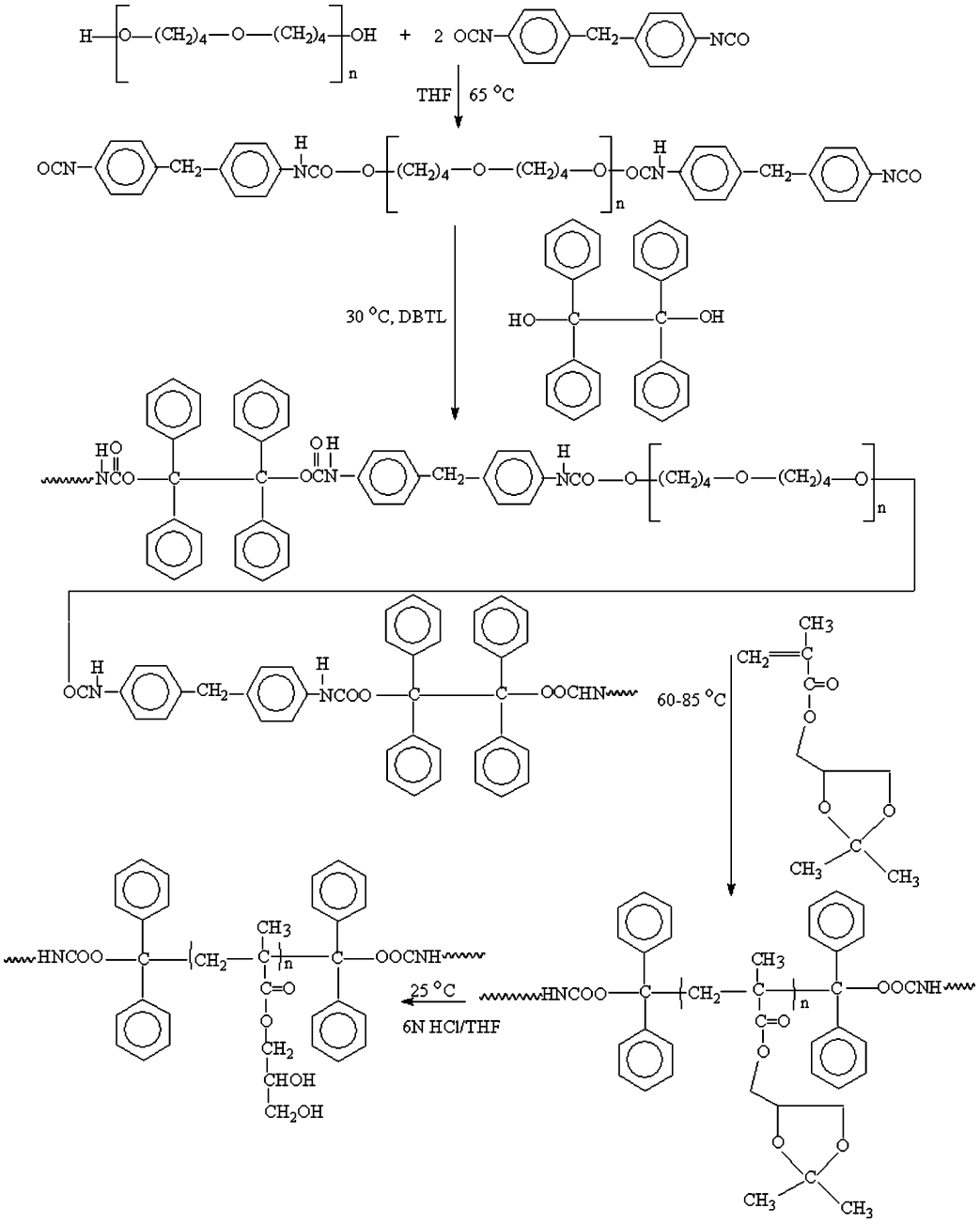

perature, samples were withdrawn at intervals of 4 h, quenched in ice-cold water to terminate the reaction, and precipitated in cold methanol (4 °C) before molecular weight and conversion measurements.

To convert the PU-*b*-PSMA to swellable PU-*b*-PGMA xerogels by selective hydrolysis, specimens were dissolved in THF and 6 N HCl (8/1 m/m ratio) followed by stirring at room temperature. Samples were taken every 30 min (to a maximum time of 4 h) and purified by dialysis against methanol, precipitated in diethyl ether, and dried in a vacuum oven at 60 °C. To ensure the selective hydrolysis of PSMA, a control PUMI sample was subjected to the same hydrolysis experiment, and molecular weight determination before and after hydrolysis gave the same value. Completion of PSMA hydrolysis was confirmed by NMR. The reaction paths for the synthesis of the block copolymer xerogels are shown in Scheme 2.

PU-*b*-PSMA polymers were synthesized with different amounts of SMA. Sample nomenclature is as follows: PU-*b*-PSMA15 means a polyurethane-*block*-poly(solketal methacrylate) with 15 wt % of poly-(solketal methacrylate) content. Similarly PU-*b*-PGMA15 means a polyurethane-*block*-poly(glycerol methacrylate) with 15 wt % of poly-(glycerol methacrylate). PU-*b*-PGMA0 was used as a control.

Characterization Methods. *Spectroscopic Analyses.* FTIR spectra were recorded by using Bruker Vector 22 spectrophotometer and ^{1}H NMR analysis was performed by Bruker AV-500 operating at 500 MHz.

Molecular Weight Determination. Gel permeation chromatography (GPC) equipped with ELSD (PL 1000), UV detector (Water 486), pump (Waters 515), and styragel columns (3 in series of pores sizes 10^5Å, 10^4Å, 10^3Å) was used to determine the molecular weight increase with reaction time for the block copolymers at a flow rate of 1 mL/min and THF as a mobile phase. Calibration was done by polystyrene standards.

Equilibrium Water Content and Swelling Kinetics Determination. Xerogel samples of 5 mm diameter disks were cut from cast films, dried at 75 °C in a vacuum oven, and weighed. The samples were then swollen in distilled water and phosphate buffered saline (PBS) at temperatures of 20, 25, 30, and 37 °C for 72 h after which samples were removed and blotted lightly with filter paper to remove excess water. The weight of the hydrated samples was then determined. The

percent equilibrium water content (EWC) of the hydrogels was calculated based on[8]

$$EWC = \frac{W_h - W_d}{W_h} \times 100 \quad (1)$$

where W_h is the weight of the hydrated sample and W_d is the dry weight of the sample. For each specimen, four independent measurements were determined and averaged. The polymer volume fraction, Φ_2, at equilibrium swelling and 37 °C was calculated from[7]

$$\phi_2 = \left(\frac{D_0}{D_1}\right)^3 \quad (2)$$

where D_0 is the diameter of the xerogel and D_1 is the diameter of swollen gel. For the swelling kinetics, the amount of water in the swelling polymer was determined at different time intervals before equilibrium swelling was reached. The swelling kinetics of the xerogels were determined according to[15]

$$f = Kt^n \quad (3)$$

where f is the fractional water uptake, K is a constant related to the hydrogel structure, t is the swelling time, and n is a number that indicates whether diffusion or relaxation controls the swelling. The fractional water content (f) is W_t/W_∞ where W_t is the weight of water in the hydrogel at time t, and W_∞ is the weight of the water at equilibrium swelling. Equation 3 is only valid for a fractional water uptake of 0.6.[15]

Dynamic Water Contact Angle. Dynamic advancing and receding water contact angles of xerogels were measured using deionized water by the Wilhelmy plate method using rectangular samples.[16] In this study, a CAHN DCA-322 analyzer operating at 25 °C and a velocity of 100 μm/s was used. For a particular xerogel, four measurements were averaged and data are expressed as mean ±SD.

DSC Measurements of Frozen and Nonfrozen Water. Quantitative information on the amounts of frozen and nonfrozen water in the hydrogels was obtained by differential scanning calorimetry (DSC 2910, TA instrument, New Castle, DE) fitted with an intercooler. The equilibrium swollen samples were cooled to −50 °C using liquid nitrogen and left to equilibrate for 10 min before heating to 40 °C at a rate of 5 °C/min. The area under the observed melting endotherms was determined and used, in conjunction with EWC, to determine the relative amounts of frozen and nonfrozen water in the hydrogel samples. From the melting enthalpy of the different hydrogel samples, the percent weight of frozen water was calculated using the equation[8]

$$W_{frozen} = \frac{\Delta H}{\Delta H_0} \times 100 \quad (4)$$

where ΔH is the melting enthalpy of the sample and ΔH_0 is the melting enthalpy of bulk water which is taken as 334 J/g. The amount of nonfrozen water can then be obtained from the difference between the EWC of the hydrogel and the calculated frozen water.

Tensile-Stress Tests and Network Parameters. The tensile strength of the hydrogels was measured by tensile testing using a sample measuring 14 mm × 3 mm, cut from the center of the cast film. The sample was placed in the jaws of an Instron model 5544 tensile tester equipped with version IX software. Since the hydrogels are likely to dehydrate during sample clamping, measurements were done inside a water bath (37 °C) fitted to the Instron at a crosshead speed of 10 mm/min and a load cell of 5 kN. Hydrogel network parameters were obtained using the modulus of elasticity, E, derived from tensile experiments and the following equations:[7]

$$\upsilon_e = \frac{G}{RT{\Phi_2}^{0.33}} = \frac{E}{3RT{\Phi_2}^{0.33}} \quad (5)$$

$$M_c = \frac{\rho}{\upsilon_e} \quad (6)$$

where G is the shear modulus, υ_e is the effective cross-link density, Φ_2 is the polymer volume fraction, R is the universal gas constant, T is the temperature, ρ is xerogel density (calculated from xerogel mass and geometric volume), and M_c is the molecular weight between cross-links.

Protein Adsorption. Quantitative single protein adsorption experiments in PBS were determined by bicinchoninic acid assay (Pierce BCA Assay Kit #23235, Rockford, IL).[17] Human serum albumin (~99% agarose gel electrophoresis), human fibrinogen (60% protein; >80% clottable protein), and γ-globulin (99% electrophoresis) were obtained from Sigma (St. Louis, MO). Hydrogel disks, 5 mm in diameter, were equilibrated in PBS for a period of 24 h and then exposed to a known concentration of human plasma proteins for 3 h at room temperature. Protein concentrations in PBS ranged from 0.01 to 1 mg/mL. Following the adsorption experiment, the hydrogel disks were rinsed 3 times (10 min each) in PBS to remove loosely bound protein. The disks were then transferred into a glass tube containing 5 mL of 2-wt % aqueous solution of sodium dodecyl sulfate (SDS) and shaken for 4 h at room temperature to elute the proteins adsorbed to the hydrogels. During screening experiments, we determined that an elution time of 4 h removed all adsorbed proteins. The amount of adsorbed protein was calculated from the concentration of proteins in the SDS solution read at 562 nm[18] and a calibration curve prepared from a pure sample of each of the target proteins measured. Four repeats (3 disks per repeat) at each concentration were measured and the average value was taken.

Platelet Adhesion. Platelet adhesion experiments were conducted according to the lactate dehydrogenase (LDH) assay.[19] The accuracy and sensitivity of this method proved to be comparable to that of radiolabeling.[19,20] Blood was drawn from healthy volunteers, and platelet-rich plasma (PRP) with cell density 1.5×10^8 cells/mL was prepared from citrated whole blood (3.8% sodium citrate; blood to citrate 9:1, v/v), by centrifugation. Xerogels of 5 mm diameter were equilibrated with PBS overnight. A total of 0.6 mL of PRP was transferred to 24-well culture plates, and the PBS equilibrated hydrogels were placed into the PRP containing wells. Incubation was carried out at 37 °C for 2 h after which the hydrogel disks were removed and rinsed with 1 mL of PBS to remove loosely attached platelets. The disks were then transferred to a glass tube and 2 mL of lysis buffer (1% Triton X 100) was added to disrupt the platelets. LDH activity of the lysate was determined by adding 0.3 mL of Monotest LDH (Boehringer, Germany). The amount of adhered platelets was calculated using a UV spectrophotometer at 340 nm from the concentration of platelets in the lysate solution. A calibration curve was prepared from the UV absorption of known platelet concentrations. Four measurements for each sample were determined, and the average value was taken.

Results and Discussions

Macroiniferter and Block Copolymer Syntheses. We have synthesized PU-*b*-PSMA by controlled radical polymerization using polyurethane macroiniferter. Table 1 summarizes the compositions of the different block copolymers synthesized with the corresponding xerogel and the molecular weight.

The FTIR spectra of TPED, PUMI, and block polymers are shown in Figure 1, from which it is clear that all of the expected peaks have appeared. The FTIR spectrum of TPED showed an −OH peak at 3500−3580 cm^{-1}. For the PUMI, the peak at 3300 cm^{-1}, a characteristic of the urethane amide bond appeared while the OH peak we observed for TPED has disappeared indicating that the chain extension reaction was completed. When the PU-*b*-PSMA copolymers were hydrolyzed to give PU-*b*-PGMA, the −NH and −OH peaks are overlapped and a broader peak between 3370 and 3400 cm^{-1} is observed. This

Table 1. Composition of PU-*b*-PSMA and the Corresponding PU-*b*-PGMA Xerogels, Molecular Weight, and Molecular Weight Distribution

parent polymer[a]	corresponding hydrogel[b]	percent weight ratio composition, %	GPC data	
			$M_n(\times 10^4)$	M_w/M_n
PU-*b*-PSMA0	PU-*b*-PGMA0	100:0	4.50	2.71
PU-*b*-PSMA15	PU-*b*-PGMA15	85:15	5.58	2.02
PU-*b*-PSMA30	PU-*b*-PGMA30	70:30	6.01	1.74
PU-*b*-PSMA40	PU-*b*-PGMA40	60:40	6.52	1.67
PU-*b*-PSMA50	PU-*b*-PGMA50	50:50	7.30	1.49

[a] PSMA content calculated based on conversion and yield during synthesis. [b] When PSMA was completely hydrolyzed.

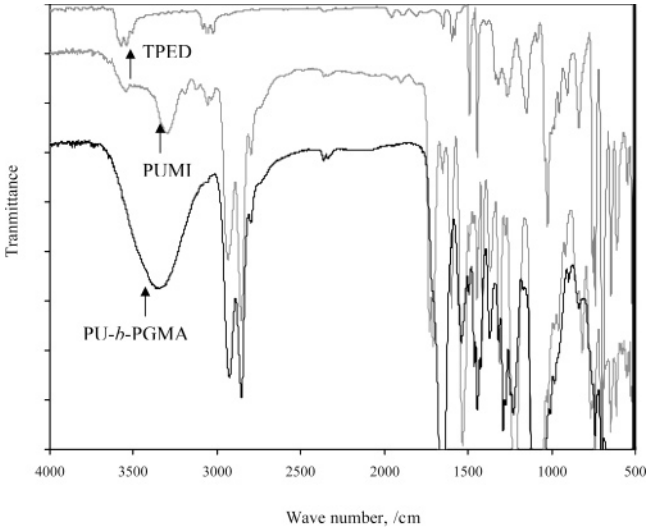

Figure 1. FTIR spectra of TPED (OH peak at 3500−3580 cm^{-1}), PUMI (NH peak at 3300 cm^{-1}), and PU-*b*-PGMA (broader and overlapped −NH and −OH peaks between 3370 and 3400 cm^{-1}).

is a confirmation of the hydroxyl groups in the PU-*b*-PGMA. The FTIR peaks of primary and secondary alcohols in PGMA block were observed at lower wavenumbers than tertiary alcohols from TPED, which is expected. Thus PU-*b*-PGMA copolymer xerogels were obtained from successfully synthesized PU-*b*-PSMA.

The PUMI used to initiate the polymerization of solketal methacrylate showed a typical "living" polymerization behavior where both molecular weight and conversion linearly increased with reaction time as presented in Figure 2. At a fixed feed composition, the conversion was highly temperature dependent. Figure 2 revealed that nearly 90% conversion was achieved within 16 h of polymerization at 85 °C compared with less than 45% conversion at 60 °C.

Braun and co-workers used TPED as a free radical initiator to polymerize a number of vinyl polymers.[21] However, TPED must be modified by reacting at least one of its hydroxyl groups to be used as an iniferter for "living" radical polymerization.[22] Since macroiniferters involve initiation, chain transfer, and/or radical termination, the rate of reaction is believed to be lower than that of the conventional free radical system.[13] This is supported by the polymerization time in Figure 2, whereby over 12 h was needed to get substantial conversion.

Effect of Hydrolysis Time on Equilibrium Water Contents of Hydrogels. The current hydrogels were obtained by the selective hydrolysis of the poly(solketal methacrylate) block to poly(glycerol methacrylate). Therefore, the equilibrium water content (EWC) is expected to be dependent on the hydrolysis

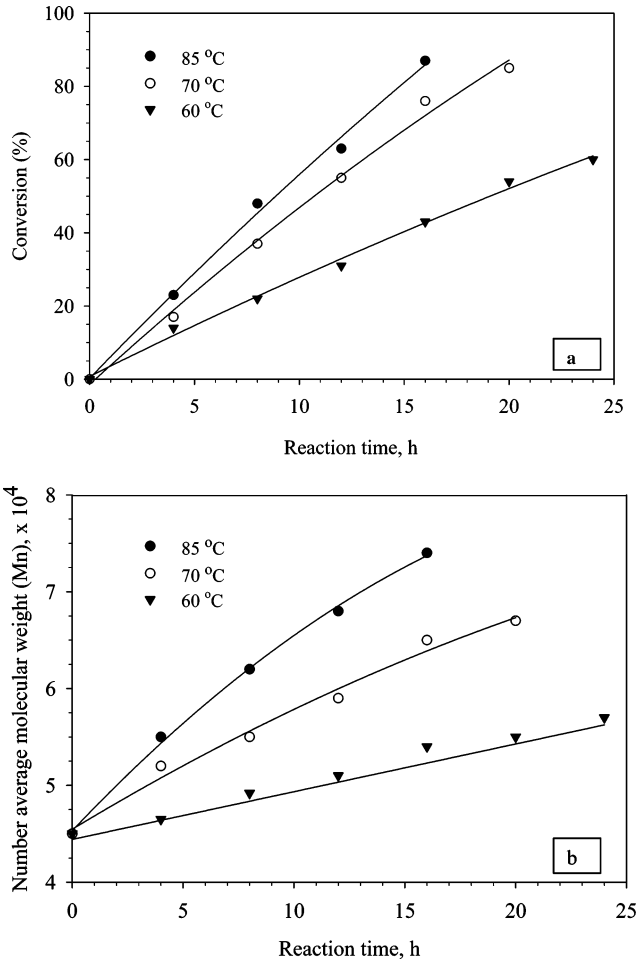

Figure 2. Conversion vs polymerization time (a) and molecular weight vs polymerization time (b) during the "living" radical polymerization of solketal methacrylate (SMA) using polyurethane macroiniferter.

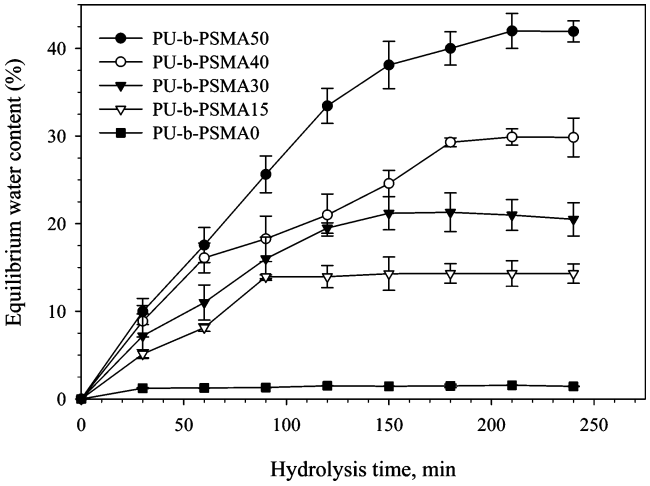

Figure 3. Effect of PU-*b*-PSMA hydrolysis time on the equilibrium water content of the corresponding PU-*b*-PGMA hydrogels at 25 °C. Data are expressed as ±SD for four independent measurements.

time. Indeed, the EWC of the PU-*b*-PGMA hydrogels increased with hydrolysis time as presented in Figure 3.

Each data point in Figure 3 is the EWC of the hydrogels at the corresponding hydrolysis time. The time required for complete hydrolysis of the PSMA block was 90 min for PU-*b*-PSMA15, whereas it was 210 min for PU-*b*-PSMA50. This was also supported by NMR analysis (data not shown). As can be seen from the figure, further hydrolysis time did not increase

Table 2. Advancing and Receding Water Contact Angles of PU-*b*-PGMA as a Function of Hydrolysis Time[a]

		hydrolysis time, min				
sample		0	60	120	180	240
PU-*b*-PGMA0	advancing	84 ± 0.42				
	receding	75 ± 0.71				
PU-*b*-PGMA15	advancing	79 ± 0.20	71 ± 1.20	61 ± 0.30	53 ± 0.72	53 ± 0.75
	receding	71 ± 0.67	62 ± 0.33	53 ± 0.34	34 ± 0.65	33 ± 0.46
PU-*b*-PGMA30	advancing	80 ± 0.83	65 ± 0.77	49 ± 0.42	46 ± 0.55	46 ± 0.52
	receding	72 ± 0.35	50 ± 0.44	43 ± 0.81	37 ± 0.46	36 ± 0.61
PU-*b*-PGMA40	advancing	81 ± 0.84	66 ± 0.62	54 ± 0.33	42 ± 0.49	41 ± 0.59
	receding	74 ± 0.62	52 ± 0.92	44 ± 0.37	33 ± 0.23	31 ± 0.81
PU-*b*-PGMA50	advancing	84 ± 0.55	64 ± 0.81	48 ± 0.17	43 ± 0.78	32 ± 0.27
	receding	75 ± 0.80	51 ± 0.42	44 ± 0.29	31 ± 0.72	20 ± 0.48

[a] Data are expressed as ±SD. Contact angles decreased as a function of hydrolysis time.

Table 3. Polymer Volume Fraction (Φ_2) at Equilibrium Swelling and the Swelling Kinetic Parameter (n)[a]

sample	Φ_2	n
PU-*b*-PGMA0	0.9873	
PU-*b*-PGMA15	0.8571	0.472
PU-*b*-PGMA30	0.7954	0.441
PU-*b*-PGMA40	0.7015	0.468
PU-*b*-PGMA50	0.5805	0.459

[a] The value of n is less than 0.5 indicating diffusion controlled swelling.

the EWC of the hydrogels. At a fixed hydrolysis time, it is also worth mentioning that the EWC was higher for those hydrogels obtained from higher amounts of PSMA than those with lower amounts. This is expected since the principal hydrophilic block is obtained by the hydrolysis of PSMA. The polyurethane macroiniferter used as a control during the hydrolysis experiment (PU-*b*-PSMA0) did not show any appreciable swelling as shown by the nearly flat line as a function of hydrolysis time. This is a clear indication that the hydrolysis was selective to the PSMA block.

Effect of Hydrolysis Time on Dynamic Water Contact Angles. Dynamic water contact angles, which are indicative of the wetting properties of the xerogels as a function of hydrolysis time,are presented in Table 2.

As the hydrolysis time increased, the polymers showed improved wetting, as evidenced by the decrease in both advancing and receding contact angles, due to the generation of hydrophilic PGMA chains. With the exception of PU-*b*-PGMA50, the contact angles reached constant value within 3 h hydrolysis time, which is in good agreement with the EWC data discussed earlier. By increasing the hydrolysis time, the decrease in particularly the receding contact angles for all samples became more significant. This is so because the advancing contact angle is sensitive to the less wettable surfaces under nonaqueous conditions, whereas the receding contact angle is more sensitive to an already wet surface.

Effect of Temperature and Soluble Salts on Swelling Behavior. At room temperature and equilibrium swelling, the polymer volume fraction (Φ_2) of the current hydrogels decreased with an increased PGMA content as presented in Table 3. This is due to the fact that an increased PGMA content led to hydrophilic polymers with higher EWC and hence lower Φ_2.

The effect of temperature on EWC and Φ_2 of the current hydrogels is shown in Figure 4. At a fixed PGMA content, a moderate increase in EWC was observed as the swelling temperature was increased from 20 to 37 °C. This observation is a characteristic of endothermic swelling. Since the swelling of the present xerogels are endothermic, one would anticipate

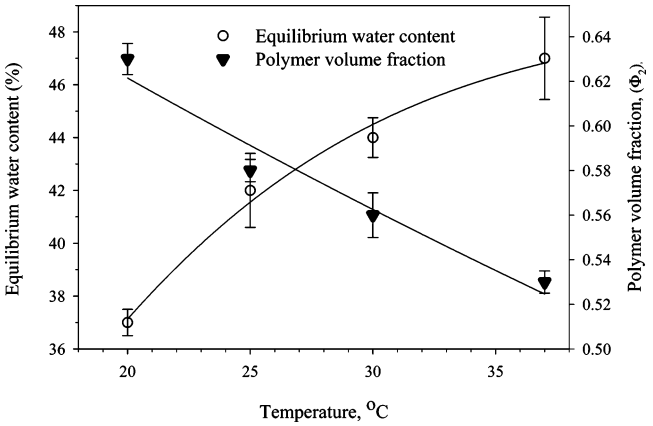

Figure 4. Effect of temperature on the equilibrium water content and polymer volume fraction for PU-*b*-PGMA50. Data are expressed as ±SD of four independent measurements.

Φ_2 to be a decreasing function of temperature. The corresponding value of Φ_2 presented in Figure 4 ascertains this expectation.

The temperature dependence of xerogel swelling has been the subject of many investigations, and depending on the nature of the molecules making the xerogel, it could increase or decrease. For instance, hydrogels based on *N*-vinyl-2-pyrolidone, poly(2-hydroxypropyl methacrylamide), and poly(ethylene oxide) showed a decreased swelling with increased temperature, whereas poly(2-hydroxyethyl methacrylate) showed both decreased and increased swelling depending on the temperature range.[23−25] Cross-linked PGMA homopolymer is known to have increased swelling when the swelling temperature is increased.[24] Since PGMA is the principal hydrophilic block in the current hydrogels, it is not surprising that we found higher swelling of the block copolymers when the temperature is increased.

The effect of soluble salts on the equilibrium water content was studied by exposing the xerogels to PBS at physiological pH. The results are presented in Figure 5. We noticed that the time needed for the hydrogels to reach an equilibrium swelling was about the same for both swelling media but equilibrium swelling was lower for PBS than that of pure water. This effect is attributed to changes in the chemical potential of water in the hydrating solution. Conversely, the decreased equilibrium swelling is explained in terms of osmotic pressure equilibrium where an increase in the number of movable counterions in the swelling solution leads to a decrease in the osmotic pressure within the sample, causing shrinkage of the hydrogel.[26]

The swelling kinetics of hydrogels is either diffusion or relaxation controlled. Swelling kinetics was determined from

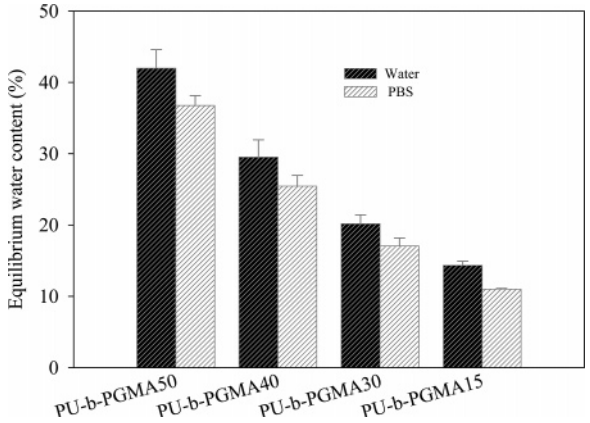

Figure 5. Effect of soluble salts on the equilibrium water content of the block copolymer hydrogels at 25 °C. Data are expressed as ±SD of four independent measurements.

Table 4. Frozen and Nonfrozen Water Quantification of the Fully Hydrolyzed Hydrogels at Equilibrium Swelling[a]

sample	EWC, % (25 °C)	frozen water, %	nonfrozen water, %
PU-*b*-PGMA0	1.40	0.30	1.10
PU-*b*-PGMA15	14.30	9.21	5.09
PU-*b*-PGMA30	20.50	12.38	7.67
PU-*b*-PGMA40	29.85	22.40	7.45
PU-*b*-PGMA50	41.95	35.12	6.83

[a] Data are average value for $n = 2$. The sum of the percent frozen and nonfrozen water equals the percent EWC.

the water up-take experiment by eq 3. Taking the natural logarithm:

$$\ln f = \ln K + n \ln t \tag{7}$$

Thus the slope of the linear plot affords the value of n, and the intercept is ln K. It has been shown that when the value of n is below 0.5 the swelling is diffusion controlled (Fickian diffusion), whereas the value of n between 0.5 and 1 indicates relaxation-controlled swelling.[15] Table 3 showed the value of n for the present hydrogels to be below 0.5, which meant that water absorption, and hence swelling, were governed by diffusion process.

DSC Quantification of Frozen and Nonfrozen Water in the Hydrogels. Frozen or nonfrozen water types are known to be present in a swollen hydrogel and the type of water influences protein adsorption and platelet activation properties of hydrogels.[27] Although frozen water is loosely absorbed, nonfrozen water is tightly bound and shows no freezing/melting transition during DSC cooling and heating processes. This indicates that water absorbed into hydrophilic polymers has somewhat different thermodynamic properties than those of water in the bulk liquid phase. The amounts of frozen and nonfrozen water in the current hydrogels are shown in Table 4.

It is interesting to note that the percentage of frozen water showed a quadratic increase ($r^2 = 0.97$) as the PGMA content in the hydrogels was increased, whereas the nonfrozen water content reached a maximum plateau value of approximately 7% above 15% PGMA content. Although one would anticipate strong water interaction with increased PGMA contents to cause higher amounts of nonfrozen water, this was not the case. As the EWC is increased, the dissociation of physical interactions such as hydrogen bonds in the hydrogel may also increase. The dissociation of the hydrogen bonds can induce an increase in the frozen water content of the hydrogels.[28] Although some researchers reported more than one type of frozen water[27,29] while others reported only one type,[8,30] the current hydrogels had only one type of frozen water.

Network and Interaction Parameters for Physically Cross-Linked Hydrogels. For many hydrogel biomaterials, effective cross-link density (υ_e) is an important aspect of their dimensional stability. Effective cross-link density for the current hydrogels was obtained from stress−strain experiments using eqs 5 and 6. From the modulus of elasticity (E), υ_e for each hydrogel was calculated using eq 5. The polymer−water interaction parameter (χ) in a swollen hydrogel was determined from the equation[31]

$$\chi = \frac{-[\ln(1 - \Phi_2) + \Phi_2 + \upsilon_e V_1(\Phi_2^{0.33} - 0.5\Phi_2)]}{\Phi_2^2} \tag{8}$$

where V_1 is the molar volume of water (1.8×10^{-5} m^3/mol). The network and interaction parameters of the current hydrogels are presented in Table 5. For all of the hydrogels, the values of E, υ_e, and χ decreased with increased amounts of PGMA. Thus, water becomes a poor "solvent" at lower PGMA contents and physical interactions assume more importance and contribute to the effective cross-link density, which is an elastic contribution.[31] Swelling occurs for the same reason that a solvent mixes with a linear polymer to form ordinary polymer solution except that the swollen gel is an elastic solution rather than a viscous. A decrease in χ with increased amounts of hydrophilic monomer means that water becomes a better "solvent". This should be the case since the hydrophobic polyurethane block is reduced when PGMA contents were increased.

Physically cross-linked hydrogels are hydrophilic networks comprised of an amorphous hydrophilic polymer phase held together by highly ordered aggregates of polymer chain segments arising from secondary molecular forces such as hydrogen bonding, van der Waals forces, and hydrophobic interactions.[6] The interest in physically cross-linked polymeric hydrogel biomaterials is obvious since the use of cross-linking agents is avoided. For instance, when a hydrogel biomaterial is used for drug delivery application, the drug has to be incorporated during the cross-linking stage that often requires either heating or ultraviolet (UV) radiation as a means of cross-linking. In the presence of heat and UV-radiation some protein drugs may lose their bioactivity and become ineffective. Since the network structure in physically cross-linked hydrogels is reversible, such aggressive conditions can be averted. In addition when the hydrogel is designed to be biodegradable, physically cross-linked hydrogels are easily degraded compared with their chemically

Table 5. Mechanical Properties and Network Parameters for PU-*b*-PGMA Hydrogels at 37 °C

sample	composition, %	E, MPa	G, MPa	v_e (mol/m^3)	M_c, Kg/mol	χ
PU-*b*-PGMA0	100:0	17.020	5.673	6.77×10^3	0.177	3.310
PU-*b*-PGMA15	85:15	2.880	0.960	1.1×10^3	1.087	1.135
PU-*b*-PGMA30	70:30	2.150	0.716	0.8×10^3	1.493	0.845
PU-*b*-PGMA40	60:40	0.770	0.256	0.27×10^3	4.345	0.568
PU-*b*-PGMA50	50:50	0.560	0.186	0.19×10^3	6.253	0.343

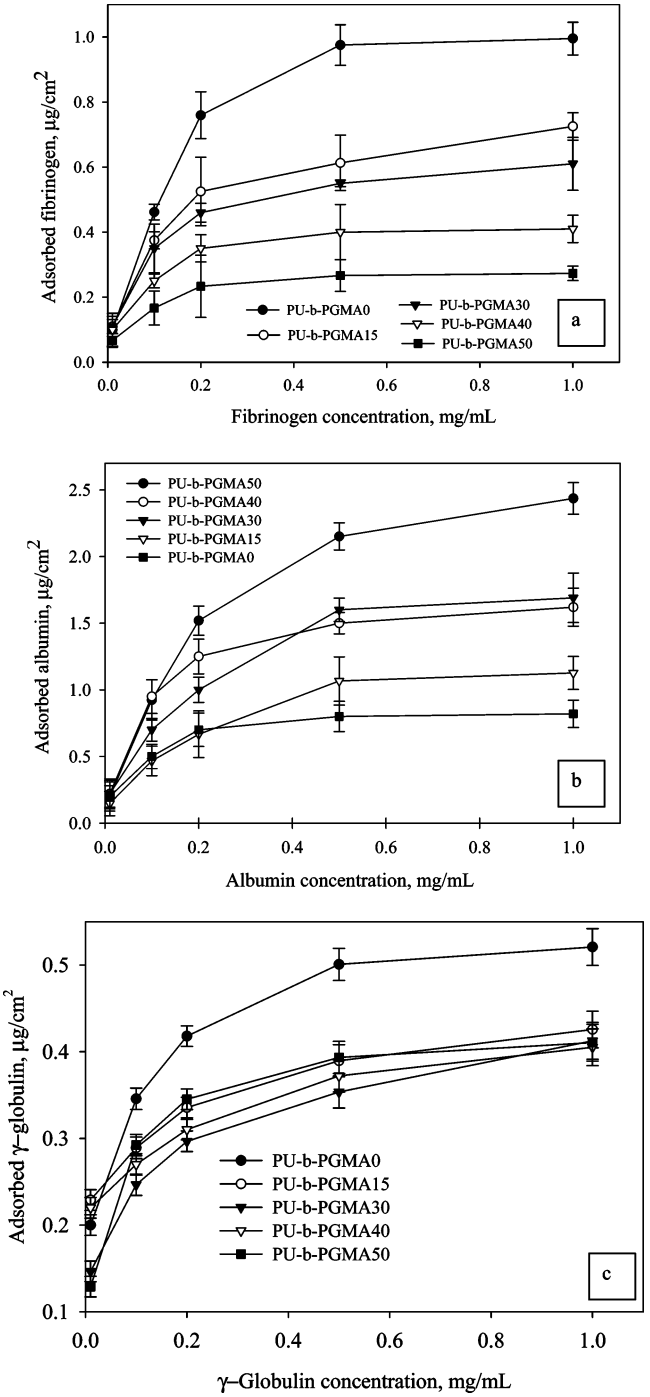

Figure 6. Single protein adsorption of PU-*b*-PGMA hydrogels from PBS as a function of protein concentration: (a) fibrinogen adsorption, (b) albumin adsorption and, (c) γ-globulin adsorption.

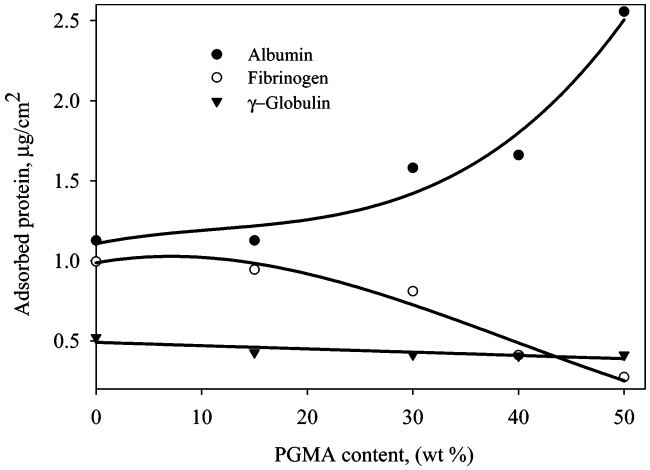

Figure 7. Single proteinadsorption of PU-*b*-PGMA as a function of PGMA content. Protein concentration was 1 mg/mL. Fibrinogen adsorption decreased while albumin adsorption increased.

cross-linked counterparts. Among physically cross-linked hydrogels, amphiphilic block copolymers are ideal candidates for biomedical applications owing to their versatility in drug delivery.[32] When block copolymers are exposed to an aqueous environment, solutions, micelles, or stable gels can be formed depending on the nature and length of the hydrophilic block. In addition to aggregation of hydrophobic chains that causes physical cross-linking, hydrogen bonding also plays a role. Since the macroiniferter polyurethane in the current hydrogels is based on PTMO, the presence of hydrogen bonding between the PTMO and urethane hard segments is obvious. It is also plausible to assume the presence of hydrogen bonding between the urethane hydrogen and the carbonyl of the PGMA that makes the current hydrogel biomaterials mechanically strong. All of the current hydrogels were soluble in most organic solvents, but when films cast from solution are placed in water or PBS, the films swell without dissolving. Furthermore, for the aqueous environment experimental conditions described, we did not observe any mass loss of the hydrogels, indicating the absence of soluble fractions.

Protein Adsorption. The protein adsorption data for the current hydrogels are presented in Figure 6a−c. Figure 6a revealed that fibrinogen adsorption was high for the control PU-*b*-PGMA0. All of the hydrogel samples adsorb significantly lower fibrinogen than the control. The adsorption data also showed that the reduction was in accordance with PGMA contents. The lowest fibrinogen adsorption value for these hydrogels was observed at 0.25μg/cm^2 for the PU-*b*-PGMA50 at 1 mg/mL protein concentration. Albumin adsorption showed the opposite behavior of fibrinogen (Figure 6b). Here, the PU-*b*-PGMA50 adsorbed the most albumin and that the adsorption decreased with decreasing PGMA contents and reached the minimum for the control. This data suggested that albumin has a higher affinity to the hydrogel surfaces than the control. This is very promising since albumin has a passivating effect and biomaterials that adsorb higher amounts of albumin are considered to be biocompatible.[33] Another possible reason hydrogels adsorb more albumin than fibrinogen may be due to absorption. When the size of the protein is relatively small, both adsorption and absorption are known to occur.[8,34]

Although there is a clear indication that the control PU-*b*-PGMA0 adsorbed more γ-globulin than the hydrogels, there is very little difference between the different hydrogels, and the effect of the PGMA content seems to play little role within the experimental ranges investigated (Figure 6c). Haigh et al.[35] reported increased γ-globulin adsorption from lauryl methacrylate-*stat*-glycerol methacrylate hydrogel networks when the glycerol methacrylate amount was increased. This difference may be caused due to the different chemistry between the polyurethane and lauryl methacrylate. The effect of PGMA content on the adsorption of proteins is summarized in Figure 7, which clearly demonstrated that fibrinogen adsorption was reduced when the amounts of PGMA was increased.

Platelet Adhesion. The platelet adhesion results of the current hydrogels are presented in Figure 8. The figure shows that the number of platelets adhered after 2 h of incubation has decreased with increased PGMA contents. The lower platelet adhesion property of the hydrogels compared with the control can be

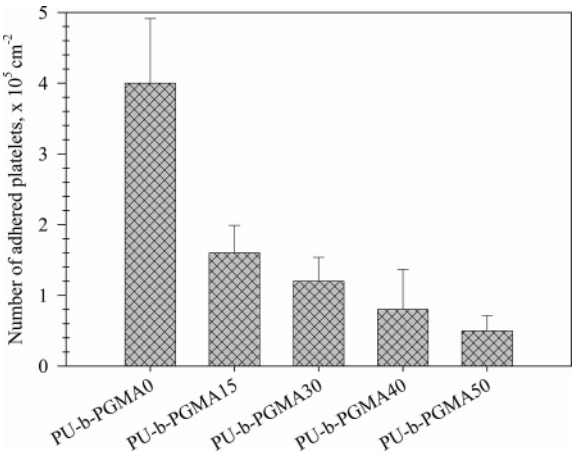

Figure 8. Effect of PGMA content (and hence equilibrium water content) on platelet adhesion for PU-*b*-PGMA hydrogels.

accounted for by the decrease in interfacial free energy between the aqueous phase and the hydrogel surface as the PGMA content was increased. This is consistent with the work of Kulik and Ikada who investigated platelet adhesion to a series of hydrogel surfaces and found that platelet adhesion decreased as the equilibrium water content of the hydrogels increased irrespective of the nature of the polymer.[36] As discussed earlier, some researchers attributed the low protein adsorption and platelet adhesion properties of hydrogels to the presence of more than one type of frozen water.[27,29] This type of water, which is observed to show a melting endotherm at lower temperatures than pure water, has been postulated to form a barrier layer.[27] Since we did not observe this type of water, we concluded that the decrease in the interfacial energy is the primary reason for the good biocompatibility of the current hydrogels. The lower number of platelets adhered to the hydrogels in conjunction with the protein adsorption data discussed above is an excellent indication that these hydrogels have a potential for biomedical applications. However, further investigation on protein adsorption from plasma and platelet adhesion in flow conditions is needed to explore the full potentials of these hydrogels.

Conclusions

We have synthesized polyurethane-*block*-poly(glycerol methacrylate) hydrogels for biomedical applications by a macroiniferter method and subsequent hydrolysis. All of the polymers synthesized using the macroiniferter method were soluble in most organic solvents, but when films cast from solution were placed in water or PBS, the films swell without dissolving. Hydrogels with equilibrium water content up to 42% were obtained by selective hydrolysis of PSMA block. In the current study, PGMA contents up to 50% were found to form stable physically cross-linked hydrogels. Both EWC and contact angle studies have shown that hydrolysis was time dependent. The current hydrogels also showed low platelet adhesion, low fibrinogen, and higher albumin adsorptions which makes them ideal candidates for coating blood-contacting devices such as catheters for hemodialysis, drug delivery, and scaffolds for tissue engineering.

Acknowledgment. The authors thank Dr. Amin Rizkalla for the useful discussion and comments on hydrogel characterization. Funding support was in part provided by the Natural Sciences and Engineering Research Council of Canada.

References and Notes

(1) Gemeinhart, R.; Guo, C. Fast Swelling Hydrogel Systems. In *Reflexive Polymers and Hydrogels − Understanding and Designing Fast Responsive Polymeric Systems*; CRC Press: Boca Raton, FL, 2004; Chapter 13.
(2) Hennink, W.; van Nostrum, C. *Adv. Drug Delivery Rev.* **2002**, *54*, 5413−36.
(3) Molina, I.; Li, S.; Martinez, M.; Vert, M. *Biomaterials* **2002**, *22*, 363−369.
(4) Liu, Y.; Huglin, M. *Polymer* **1995**, *36*, 1715−1718.
(5) Liu, Y.; Huglin, M. *Polym. Int.* **1995**, *37*, 63−67.
(6) Devine, D.; Higginbotham, C. *Polymer* **2003**, *44*, 7851−7860.
(7) Muratore, L.; Davis, T. *J. Polym. Sci. Polym. Chem.* **2000**, *38*, 810−817.
(8) Mequanint, K.; Sheardown, H. *J. Biomater. Sci. Polym. Ed.* **2005**, *10*, 1303−1318.
(9) Petrini, P.; Tanzi, M. *J. Mater. Sci. Mater. Med.* **1999**, *10*, 635−639.
(10) Johnson, B.; Bauer, J.; Niedermaier, D.; Crone, W.; Beebe, D. *Exp. Mech.* **2004**, *44*, 21−28.
(11) Jagur-Grodzinski, J. *React. Funct. Polym.* **2001**, *49*, 1−54.
(12) Sundar, S.; Tharanikkarasu, K.; Dhathathreyan, A.; Radhakrishnan, G. *Colloid Polym. Sci.* **2002**, *280*, 915−921.
(13) Otsu, T.; Matsumoto, A. *Adv. Polym. Sci.* **1998**, *136*, 75−137.
(14) Oguchi, K.; Sanui, K.; Ogata, N. *Polym. Eng. Sci.* **1990**, *30*, 449−452.
(15) Khare, A.; Peppas, N. *Biomaterials* **1995**, *16*, 559−567.
(16) Bona, A.; Shen, C.; Anusavice, K. *Dent. Mater.* **2004**, *20*, 338−344.
(17) Higuchia, A.; Sugiyamaa, K.; Yoona, B.; Sakuraib, M.; Haraa, M.; Sumitac, M.; Sugawarac, S.; Shiraic, T. *Biomaterials* **2003**, *24*, 3235−3245.
(18) Brown, R.; Jarvis, K.; Hyland, K. *Anal. Biochem.* **1989**, *180*, 136−139.
(19) Tamada, Y.; Kulik, E.; Ikada, Y. *Biomaterials* **1995**, *16*, 259−261.
(20) Park, J.; Gemmell, C.; Davies, J. *Biomaterials* **2001**, *22*, 2671−2682.
(21) Braun, D.; Becker, K. *Ind. Eng. Chem. Prod. Res. Dev.* **1971**, *10*, 386-388.
(22) Chen, X.; Qiu, K.; Swift, G.; Westmoreland, D.; Wu, S. *Euro. Polym. J.* **2000**, *36*, 1547−1554.
(23) Okoroafor, E. *J. Phys. D: Appl. Phys.* **1999**, *32*, 2454−2461.
(24) Nierzwicki, W.; Prins, W. *J. Appl. Polym. Sci.* **1975**, *19*, 1885−1892.
(25) Cho, H.; Noh, S. *J. Ind. Eng. Chem.* **2000**, *6*, 19−24.
(26) Kim, S.; Shin, S.; Lee, S.; Kim, I.; Kim, SI. *Smart Mater. Struct.* **2004**, *13*, 1036−1039.
(27) Tanaka, M.; Mochiziki, A.; Ishii, N.; Motomura, T.; Hatakeyama, T. *Biomacromolecules* **2002**, *3*, 36−41.
(28) Kim, S. J.; Park, SJ.; Kim, SI. *Smart Mater. Struct.* **2004**, *13*, 317−322.
(29) Zhang, J.; Teng, H.; Zhou, X.; Shen, D. *Polym. Bull.* **2002**, *48*, 277−282.
(30) Mueller-Plathe, F. *Macromolecules* **1998**, *31*, 6721−6723.
(31) Flory, P. *Principles of Polymer Chemistry*; Cornell University Press: Ithica, NY, 1953; p578.
(32) Adams, M.; Lavasanifar, A.; Kwon, G. *J. Pharm. Sci.* **2003**, *92*, 1343−1355.
(33) Vermette, P., Griesser, H., Laroche, G., Guidoin, R., Eds.; *Biomedical Applications of Polyurethanes*; Landes Bioscience: Austin, TX, 2002; Chapter 6.
(34) Garrett, Q.; Chatelier, R.; Griesser, H.; Milthorpe, B. *Biomaterials* **1998**, *19*, 2175−2186.
(35) Haigh, R.; Rimmer, S.; Fullwood, N. *Biomaterials* **2000**, *21*, 735−739.
(36) Kulik, E.; Ikada, Y. *J. Biomed. Mater. Res.* **1996**, *30*, 294−304.

BM0507047